DOI: 10.19884/j.1672-5220.202310001

# Semi-Active Sound Absorption Method with Acoustic Impedance Matching

ZHU Congyun*, ZHANG Shaoqi, DING Guofang
School of Intelligent Mechatronics Engineering (School of Industrial Design), Zhongyuan University of Technology, Zhengzhou 450007, China

**Abstract: The active sound absorption technique excels in mitigating low-frequency sound waves, yet it falls short when dealing with medium and high-frequency sound waves. To enhance the sound-absorbing effect of medium and high-frequency sound waves, a novel semi-active sound absorption method has been introduced. This method modulates the surface impedance of a loudspeaker positioned behind the sound-absorbing material, thereby altering the sound absorption coefficient. The theoretical sound absorption coefficient is calculated using MATLAB and compared with the experimental one. Results show that the method can effectively modulates the absorption coefficient in response to varying incident sound wave frequencies, ensuring that it remains at its peak value.**

**Keywords**: acoustic impedance; semi-active sound absorption; rigid wall; cavity depth; sound absorption coefficient
**CLC number**: TB53 **Document code**: A
**Article ID**: 1672-5220(2025)01-0064-07

Open Science Identity (OSID)

## 0 Introduction

Semi-active sound absorption has gained significant attention in recent years. Guicking et al.[1] adopted two loudspeakers as primary and secondary sound sources, respectively, and connected a sensor to an acoustic impedance controller to match the acoustic impedance at the surface of the secondary loudspeaker with the air impedance for active sound absorption. However, the optimality of the sound-absorbing effect was not assessed. Orduña-Bustamante et al.[2] used the transfer function method to detect the sound pressure and frequency of the incident sound wave, and then used the active control body to reduce the reflected sound pressure. Yet, the potential error introduced by the transfer function method was overlooked. Belov et al.[3] proposed and studied an active-passive absorber. However, they did not delve into the sound absorption performance across different frequencies. Selamat et al.[4] developed a semi-active panel design for a sound absorber, and experimentally verified the maximum sound absorption coefficient with various perforation sizes. The design was effective for single sound waves in medium and low-frequency ranges, but had limited effectiveness in the broad frequency range. Researchers used the multi-physics simulation software COMSOL and the finite element method to study the acoustic characteristics of a direct-through perforated tube silencer with multiple layers of sound-absorbing materials[5-6]. Zhang et al.[7] studied the combined active and passive sound absorption of porous panels. Despite these efforts, research on semi-active sound absorption remains relatively limited.

In this paper, the sound absorption coefficient is maximized by changing the cavity depth of the sound-absorbing material. In order to obtain a higher absorption coefficient across all frequencies, a novel semi-active sound absorption method is proposed.

## 1 Semi-Active Sound Absorption Principle by Varying Cavity Depth

Figure 1 illustrates the structure of the semi-active sound absorption system. The distance between the two microphones is denoted as $d$, and the distance from the sound-absorbing material is also $d$. The thickness of the sound-absorbing material is $D_1$, the depth of the cavity from the rigid wall is $D_2$, the coordinate origin $O$ is at the critical point between the cavity and the sound-absorbing material, and the positive direction is vertically inward along the $x$ axis.

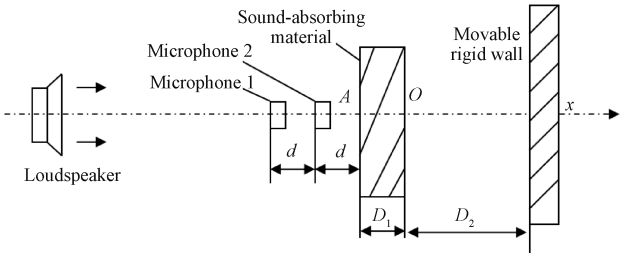


Fig. 1 Structure of semi-active sound absorption system

Received date: 2023-10-06
Foundation item: National Natural Science Foundation of China (No. 51705545)
* Correspondence should be addressed to ZHU Congyun, email: zcy711126@163.com
Citation: ZHU C Y, ZHANG S Q, DING G F. Semi-active sound absorption method with acoustic impedance matching[J]. *Journal of Donghua University (English Edition)*, 2025, 42(1): 64-70.

The acoustic impedance at $x$ along the horizontal axis is

$$Z_x = \rho c \coth\left(\zeta - \frac{\mathrm{j}\omega x}{c}\right), \tag{1}$$

where $\rho$ is the density of the sound-absorbing material; $c$ is the sound speed within the sound-absorbing material under various sound wave conditions; $\rho c$ denotes the acoustic impedance of the material; $\zeta$ is a complex number; $\omega$ is the angular frequency of the sound wave.

When $x = 0$,

$$Z_{x0} = \rho c \coth \zeta = \rho_0 c_0 \coth \frac{\mathrm{j}\omega D_2}{c_0}, \tag{2}$$

where $\rho_0$ is the air density; $c_0$ is the sound speed in air; $\rho_0 c_0$ denotes the acoustic impedance of air. The acoustic impedance[8] at the point $A$ ($x = -D_1$) on the sound-absorbing material surface is

$$Z_A = \rho c \coth\left(\zeta + \frac{\mathrm{j}\omega D_1}{c}\right). \tag{3}$$

Expand Eq. (3):

$$Z_A = \frac{\rho_0 \rho c_0 c \coth \dfrac{\mathrm{j}\omega D_1}{c} \coth \dfrac{\mathrm{j}\omega D_2}{c_0} + (\rho c)^2}{\rho c \coth \dfrac{\mathrm{j}\omega D_1}{c} + \rho_0 c_0 \coth \dfrac{\mathrm{j}\omega D_2}{c_0}}. \tag{4}$$

The reflection coefficient of the sound-absorbing material surface $R$ can be obtained from Eq. (4):

$$R = \frac{Z_A - \rho_0 c_0}{Z_A + \rho_0 c_0}. \tag{5}$$

The sound absorption coefficient of the sound-absorbing material surface $\alpha$ is obtained:

$$\alpha = 1 - |R|^2. \tag{6}$$

It can be seen from Eqs. (4) – (6) that when sound waves with different frequencies are incident, the acoustic impedance of the sound-absorbing material surface can be adjusted by changing the cavity depth of the sound-absorbing material. To achieve the highest sound absorption coefficient, it is essential that the acoustic impedance of the sound-absorbing material surface matches that of air, namely impedance matching.

When $D_1 = 30$ mm, $\rho_0 = 1.21$ kg/m$^3$, $c_0 = 334$ m/s, and the incident sound wave frequencies $f$ are 150, 250, 350 and 450 Hz, respectively, the relationship between $\alpha$ and $D_2$ behind the sound-absorbing material is obtained from the experiment (shown in Fig. 2).

Figure 3 displays the relationship between $D_2$ and $f$ at the highest sound absorption coefficient. It is concluded that for incident sound waves with different frequencies, the sound absorption coefficient of the sound-absorbing material can be optimized by adjusting the position of the rigid wall and continuously altering the cavity depth.

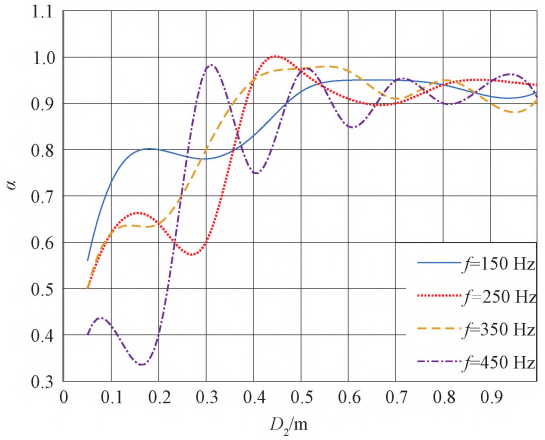


Fig. 2 Relationship between $\alpha$ and $D_2$ at various incident sound wave frequencies

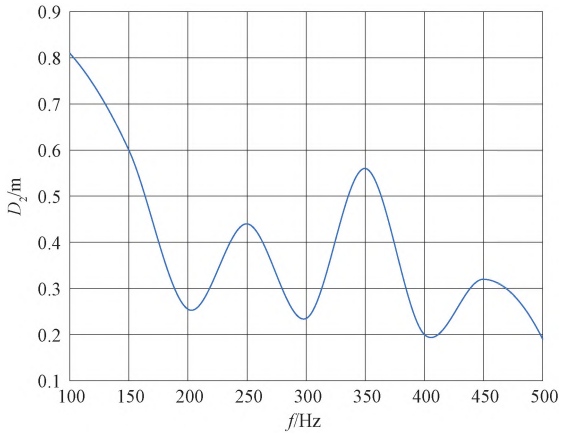


Fig. 3 Relationship between $D_2$ and $f$ at the highest $\alpha$

It can be seen from Figs. 2 and 3 that this method is effective for the sound absorption in the medium and low-frequency ranges, but has limited effectiveness in the broad frequency range. Consequently, a novel semi-active sound absorption method to adjust the acoustic impedance is studied in order to obtain a higher sound absorption coefficient at all frequencies.

## 2 Semi-Active Sound Absorption Method with Impedance Controller for Acoustic Impedance Adjustment

### 2.1 Semi-active sound absorption principle with impedance controller for acoustic impedance adjustment

The impedance arrangement in the semi-active sound absorption system with the impedance controller (the

controllable system for short) is shown in Fig. 4. The surface acoustic impedance of the sound-absorbing material $Z_1$ can be expressed by the acoustic impedance of the sound-absorbing material $\rho c$ and that of the sound-absorbing material back $Z_2$:

$$Z_1 = \rho c \frac{Z_2 \cosh(\gamma D_1) + \rho c \sinh(\gamma D_1)}{Z_2 \sinh(\gamma D_1) + \rho c \cosh(\gamma D_1)}, \quad (7)$$

where $\gamma$ is the wavenumber of sound propagation. Denote the distance between the back surface of the sound-absorbing material and the loudspeaker as the cavity depth $D_2$, therefore

$$Z_2 = \rho_0 c_0 \frac{Z_3 \cosh(kD_2) + \rho_0 c_0 \sinh(kD_2)}{Z_3 \sinh(Dd_2) + \rho_0 c_0 \cosh(kD_2)}, \quad (8)$$

where $k$ is the propagation wavenumber of sound waves, and $k = \omega / c_0$; $Z_3$ is the radiation impedance of the loadspeaker surface. When $Z_1$ is consistent with $\rho_0 c_0$, the sound absorption coefficient of the sound-absorbing material is maximum:

$$Z_1 = \rho_0 c_0. \quad (9)$$

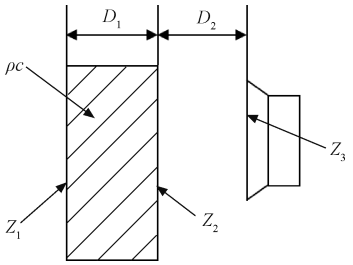


Fig. 4 Diagram of impedance arrangement

The impedance adjustable loudspeaker is a moving-coil loudspeaker. The commonly used moving-coil loudspeaker can be approximated as a concentrated parameter system at the low frequency[9]. According to the electroacoustic analogy method, the circuit simulation is drawn as shown in Fig. 5, where $E_g$ is the electromotive force of the signal source[10]; $R_e$ is the direct current resistance of the voice coil, which constitutes the static impedance of the loudspeaker electrical part $Z_0$, the same as the acoustic impedance of air, and $Z_0 = R_e$; $R_{ms}$ is the mechanical impedance of the support system; $M_{ms}$ is the equivalent mass of the loudspeaker; $C_{ms}$ is the equivalent force of the loudspeaker, and constitutes the mechanical impedance of the loudspeaker vibration part $Z_{ms}$ ($Z_{ms} = R_{ms} + j\omega M_{ms} + 1/(j\omega C_{ms})$); $B$ is the magnetic field strength of the coil gap; $L$ is the length of the voice coil wire; $BL$ is the electromechanical conversion coefficient of the loudspeaker; $S_d$ is the effective vibration area of the loudspeaker; $Z_a$ is the loudspeaker surface impedance, and $Z_a = Z_3$.

With $R_{ms} = R_{at}$, $M_{ms} = M_{as}$ and $C_{ms} = C_{as}$, the equivalent circuit diagram of the moving-coil loudspeaker shown in Fig. 5 could be simplified as an acoustic element diagram as shown in Fig. 6.

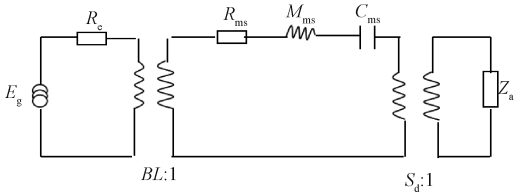


Fig. 5 Equivalent circuit diagram of moving-coil loudspeaker

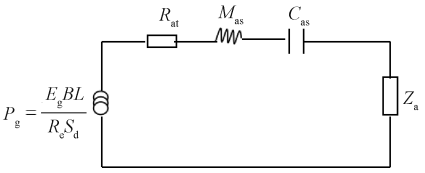


Fig. 6 Equivalent circuit diagram of moving-coil loudspeaker with acoustic elements

From Figs. 5 and 6, the following relationships are obtained:

$$C_{as} = S_d^2 C_{ms}, \quad (10)$$

$$R_{as} = S_d^{-2} R_{ms}, \quad (11)$$

$$M_{as} = S_d^{-2} M_{ms}, \quad (12)$$

$$P_g = \frac{E_g BL}{R_e S_d}, \quad (13)$$

$$R_{at} = R_{as} + \frac{B^2 L^2}{(R_g + R_e) S_d^2} = S_d^{-2} R_{ms} + \frac{B^2 L^2}{(R_g + R_e) S_d^2}. \quad (14)$$

The loudspeaker impedance $Z_a$ is equivalent to the capacitance $C_{ab}$. The frequency response[11] of the loudspeaker $G(s)$ is

$$G(s) = \frac{Z(s)}{U(s)} = \frac{s^2 M_{as} C_{as} C_{ab}}{s^2 M_{as} C_{as} C_{ab} + s R_{at} C_{as} C_{ab} + C_{as} + C_{ab}}, \quad (15)$$

where $s$ is the sound pressure area; $Z(s)$ is the intensity of the output sound at different frequencies; $U(s)$ is the input signal power.

Convert Eq. (15) into the Fourier transform form:

$$G(j\omega) = \frac{Z(j\omega)}{U(j\omega)} = \frac{-\omega^2 M_{as} C_{as} C_{ab}}{-\omega^2 M_{as} C_{as} C_{ab} + j\omega R_{at} C_{as} C_{ab} + C_{as} + C_{ab}}, \quad (16)$$

$$Z(j\omega) = \frac{-\omega^2 M_{as} C_{as} C_{ab}}{-\omega^2 M_{as} C_{as} C_{ab} + j\omega R_{at} C_{as} C_{ab} + C_{as} + C_{ab}} U(j\omega). \quad (17)$$

### 2.2 Principle of measuring sound absorption coefficient with two microphones

The time delay method[12] was used to analyze the sound absorption coefficient measured by two microphones, as shown in Fig. 7. The Laplace transform of the sound pressures at microphones 1 and 2 $p_1$ and $p_2$ can be obtained:

$$p_1(s) = p_i(s) + p_r(s)e^{-4\tau s}, \quad (18)$$

$$p_2(s) = p_i(s)e^{-\tau s} + p_r(s)e^{-3\tau s}, \quad (19)$$

where $\tau$ is time; $p_i$ is the incident sound pressure; $p_r$ is the reflected sound pressure.

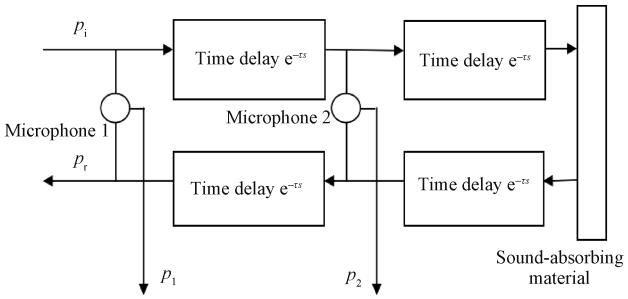


Fig. 7 Schematic diagram of time delay method

The Laplace transform of the reflection coefficient $R(s)$ can be expressed as

$$R(s) = \frac{p_r(s)}{p_i(s)}. \quad (20)$$

Define $x(t)$ and $y(t)$ as

$$x(t) = p_2(t) - p_1(t-\tau), \quad (21)$$

$$y(t) = p_1(t) - p_2(t-\tau). \quad (22)$$

Convert Eqs. (21) and (22) into the Laplace transform forms:

$$X(s) = p_2(s) - p_1(s)e^{-\tau s}, \quad (23)$$

$$Y(s) = p_1(s) - p_2(s)e^{-\tau s}. \quad (24)$$

Substituting Eqs. (18) and (19) into Eq. (23) yields:

$$X(s) = p_r(s)e^{-3\tau s} - p_r(s)e^{-5\tau s} = p_r(s)e^{-3\tau s}(1 - e^{-2\tau s}). \quad (25)$$

Substituting Eqs. (18) and (19) into Eq. (24) yields:

$$Y(s) = p_i(s) - p_i(s)e^{-2\tau s} = p_i(s)(1 - e^{-2\tau s}). \quad (26)$$

From Eqs. (20), (25) and (26), we obtain

$$R(s) = \frac{X(s)}{Y(s)}e^{3\tau s}. \quad (27)$$

The acoustic impedance of the sound-absorbing material surface $R$ can be obtained by inverse Laplace transform on Eq. (27):

$$R = L^{-1}\{R(s)\} = L^{-1}\left\{\frac{p_r(s)}{p_i(s)} = \frac{X(s)}{Y(s)}e^{3\tau s}\right\}, \quad (28)$$

where $L^{-1}$ is the inverse Laplace transform. Then, the sound absorption coefficient of the sound-absorbing material surface $\alpha$ is obtained.

### 2.3 Control principle and algorithm

The semi-active sound absorption system with the impedance controller is shown in Fig. 8. The impedance controller is mainly composed of two microphones, a sound-absorbing material and a control loudspeaker. The single-frequency or wide-frequency signals are emitted by a computer, amplified by a power amplifier and converted into sound waves by a loudspeaker to enter an impedance controller. Sound pressure signals are collected by using a signal acquisition, and are introduced into the computer. Then the acquired data are processed by using MATLAB software programs to obtain the sound absorption coefficient of the material[13-14].

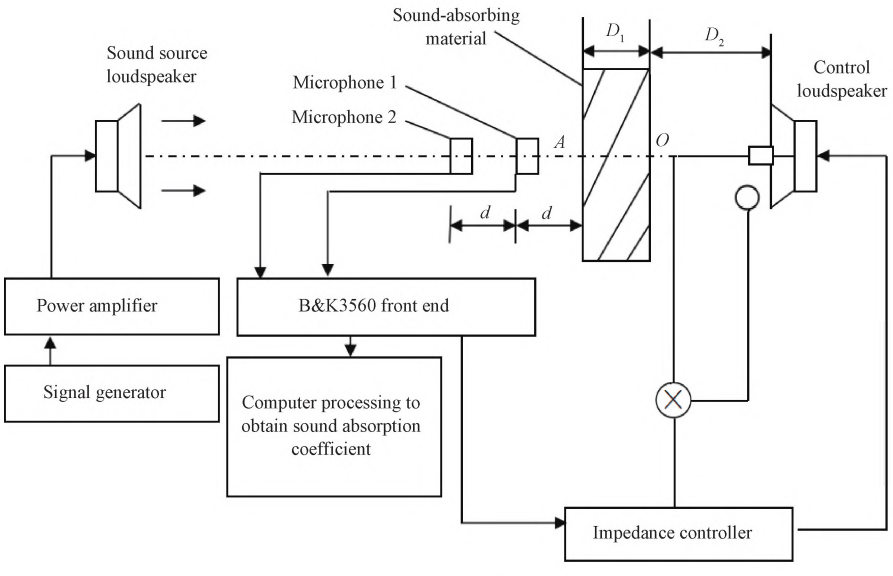


(a)

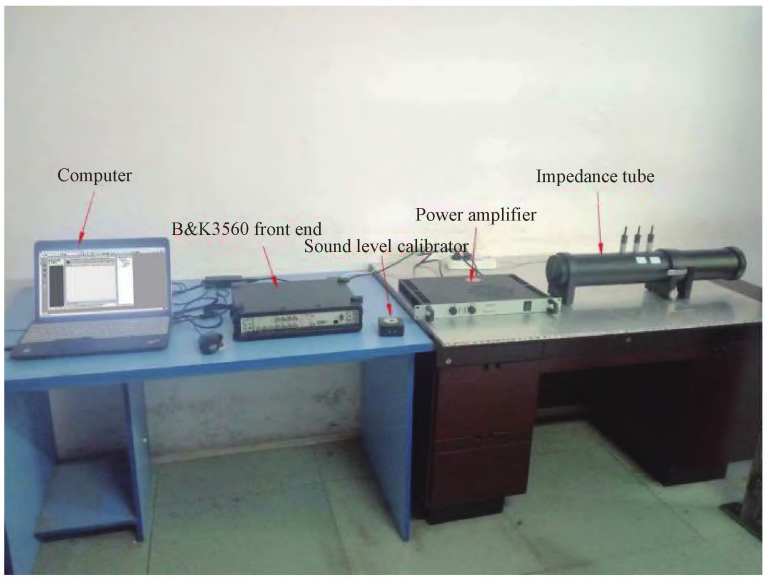


(b)

Fig. 8 Structure of semi-active sound absorption system with impedance controller: (a) schematic diagram; (b) experimental instrument

This control system is a feedback control system and the proportional-integral-differential (PID) control algorithm is adopted. The specific PID control experiment flow is shown in Fig. 9.

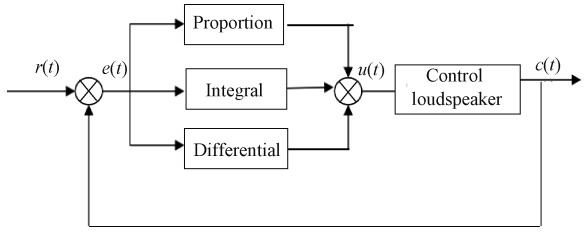


Fig. 9 Principle block diagram of conventional PID control system

The PID controller is a linear controller. The error $e(t)$ is determined based on the constant value $r(t)$ and the actual output value $c(t)$:

$$\begin{cases} e(t) = r(t) - c(t), \\ r(t) = Z_0, \\ c(t) = \dfrac{P(t)}{V(t)}, \end{cases} \tag{29}$$

where $Z_0 = \rho_0 c_0$; $V(t)$ is the sound speed of the loudspeaker surface; $P(t)$ is the sound pressure on the loudspeaker surface. The proportion (P), integral (I) and differential (D) of the error are linearly combined to form a controllable variable to control the loudspeaker:

$$u(t) = K_{\mathrm{P}}\left[e(t) + \frac{1}{T_{\mathrm{I}}}\int e(t)\,\mathrm{d}t + T_{\mathrm{D}}\frac{\mathrm{d}e(t)}{\mathrm{d}t}\right], \tag{30}$$

where $u(t)$ is control quantity; $K_{\mathrm{P}}$ is the proportional constant; $T_{\mathrm{I}}$ is the integral time constant; $T_{\mathrm{D}}$ is the differential time constant.

In the form of a transform function, there is

$$G(s) = \frac{U(s)}{e(s)} = K_{\mathrm{P}}\left(1 + \frac{1}{T_{\mathrm{I}}s} + T_{\mathrm{D}}s\right), \tag{31}$$

where $G(s)$ is the result of the transform function.

Since computer control is a kind of sampling control, it can only calculate the control quantity according to the differential value of sampling time. Thus, Eq. (31) cannot be used directly, and a discrete process is needed. Denote that the sampling period is $T$, and the sampling number is $k$, the discrete serial number is $j$, a series of sampling time points $kT$ are used instead of continuous time $t$, the sum equation is used instead of integral, and the increment is used instead of derivative:

$$\int_0^t e(t)\,\mathrm{d}t \approx T\sum_{j=0}^{k-1} e(jT) = T\sum_{j=0}^{k-1} e(j), \tag{32}$$

$$\frac{\mathrm{d}e(t)}{\mathrm{d}t} \approx \frac{e(kT) - e((k-1)T)}{T}. \tag{33}$$

Obviously, the sampling period $T$ must be short enough to ensure sufficient accuracy in the discrete process described above. For simplicity, $e(kT)$ is written as $e(k)$, and Eqs. (32) and (33) are substituted into Eq. (30) to obtain the discrete PID expression:

$$u(k) = K_{\mathrm{P}}\left\{e(k) + \frac{T}{T_I}\sum_{j=0}^{k-1} e(j) + \frac{T_D}{T}[e(k) - e(k-1)]\right\}, \tag{34}$$

where $u(k)$ is the computer output at the $k$th sampling time; $e(k)$ is the deviation value input at the $k$th sampling time; $e(k-1)$ is the deviation value input at the $(k-1)$th sampling time.

$u(k)$ is the total output by the computer, and

directly controls the actuator. $z$ transformation is a mathematical transformation of the discrete sequence. From the $z$ transformation:

$$\begin{cases} Z(u(k)) = U(z), \\ Z(e(k)) = E(z), \\ Z(e(k-1)) = z^{-1}E(z), \\ Z\sum_{j=0}^{k} e(j) = \dfrac{1}{1-z^{-1}}E(z). \end{cases} \tag{35}$$

Substituting Eq. (35) into Eq. (34), the $z$ transformation of Eq. (34) is obtained:

$$U(z) = K_P\{E(z) + \frac{T}{T_I(1-z^{-1})}E(z) + \frac{T_D}{T}[E(z) - z^{-1}E(z)]\}. \tag{36}$$

From Eq. (36), the $z$ transformation of the PID controller is

$$D(z) = \frac{U(z)}{E(z)} = K_P\left[1 + \frac{T}{T_I(1-z^{-1})} + \frac{T_D}{T}(1-z^{-1})\right]. \tag{37}$$

### 2.4 Numerical calculation

The theoretical sound absorption coefficient was calculated using MATLAB and compared with the experimental one, as shown in Fig. 10. The theoretical sound absorption coefficient before adjusting impedance is low when the incident sound wave is in medium and low-frequency ranges, while it is high when the incident sound wave is in the high-frequency range. After adjusting the impedance, the sound absorption coefficient of medium and low-frequency incident sound waves is obviously improved from about 0.40 to about 0.95; but for the high-frequency incident sound wave, the improvement is not obvious, and the sound absorption coefficient of the sound-absorbing material itself is high. Experimental verification and theoretical calculation results are basically consistent.

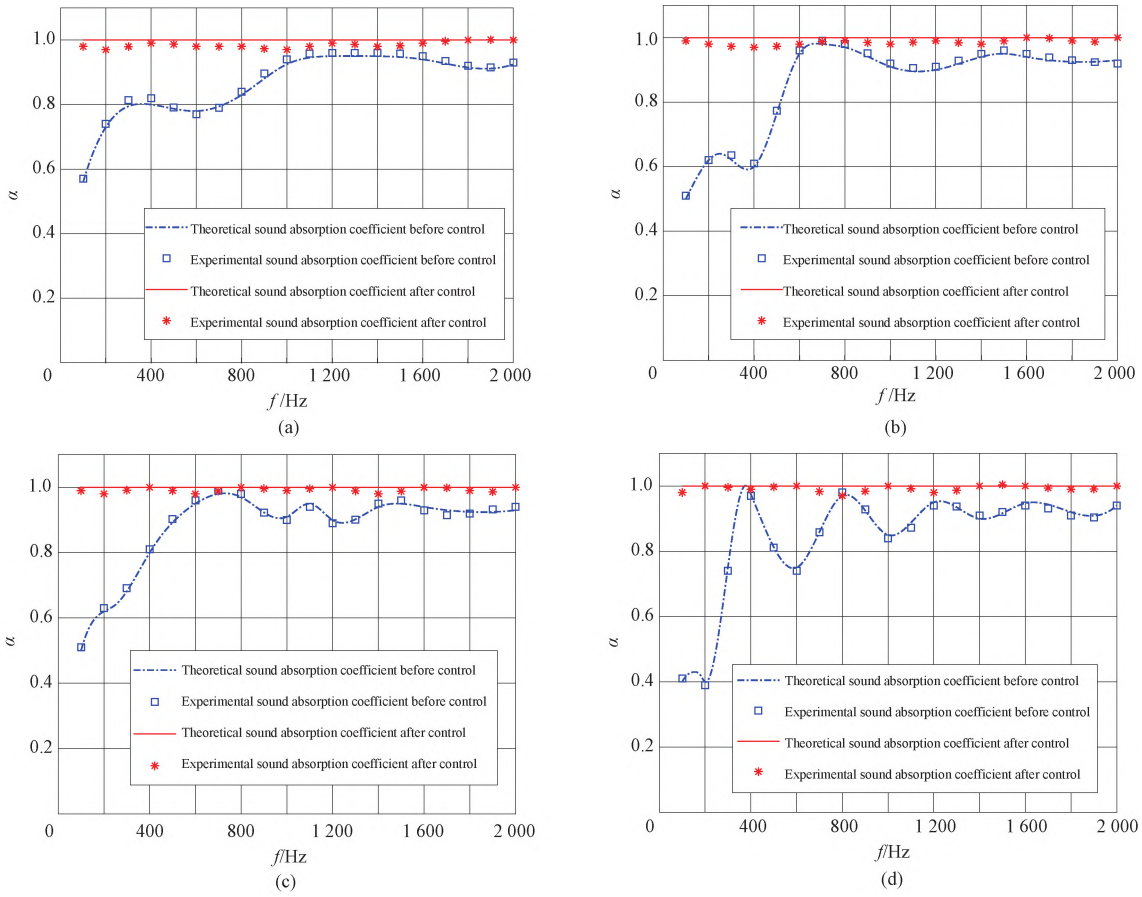


Fig. 10 Comparison of sound absorption coefficient: (a) $D_2$ = 150 mm; (b) $D_2$ = 250 mm; (c) $D_2$ = 350 mm; (d) $D_2$ = 450 mm

## 3 Conclusions

A novel semi-active sound absorption method is introduced to enhance the sound-absorbing effect of medium and high-frequency sound waves. This method modulates the surface impedance of a control loudspeaker positioned behind the sound-absorbing material, thereby altering the sound absorption coefficient. When the method is used for low-frequency incident sound waves, the sound absorption coefficient is obviously improved from about 0.40 to about 0.95; when it is used for the

high-frequency incident sound waves, the sound absorption coefficient is basically stable at around 0.95, with the good sound-absorbing effect of the sound-absorbing material itself. Therefore, it is feasible to adjust the impedance to optimize the sound absorption coefficient.

## References


[1] GUICKING D, KARCHER K. Active impedance control for one-dimensional sound[J]. *Journal of Vibration and Acoustics*, 1984, 106(3): 393-396.

[2] ORDUÑA-BUSTAMANTE F, NELSON P A. An adaptive controller for the active absorption of sound[J]. *The Journal of the Acoustical Society of America*, 1992, 91(5): 2740-2747.

[3] BELOV V D, MIGUN Y G, ORLOV A I. A hybrid active-passive sound absorber [J]. *Acoustical Physics*, 2012, 58(4): 381-386.

[4] SELAMAT N S S, TAHIR M F M, ZULKIFLI R, et al. Development of semi-active panel design for sound absorption [J]. *Applied Mechanics and Materials*, 2014, 663: 421-425.

[5] ZHU C Y, LIU R J. Theoretical calculation and analysis of muffler based on multilayer sound absorbing materials [J]. *Journal of Donghua University (English Edition)*, 2022, 39(1): 40-54.

[6] LIU R J, ZHU C Y, DING G F, et al. Calculation and analysis of acoustic characteristics of straight-through perforated pipe muffler based on multilayer sound absorbing material [J]. *Journal of Donghua University (English Edition)*, 2023, 40(5): 506-514.

[7] ZHANG R Q, ZHU C Y, DING G F, et al. Active absorption of perforated plate based on airflow [J]. *Journal of Donghua University (English Edition)*, 2022, 39(6): 590-596.

[8] ZHU C Y. Research on theories and methods of active sound absorption[D]. Wuhan: Huazhong University of Science and Technology, 2005. (in Chinese)

[9] HOU H, YANG J H, L H, et al. An impedance-based control system and its application in active noise control, part Ⅱ: electro-impedance theory and measurement [J]. *Journal of Northwestern Polytechnic University*, 2001(2): 246-250. (in Chinese)

[10] ZHU C Y, WU R, HUANG B X. et al. Sound character calculation and analysis of sound barrier based on acoustoelectric analogy[J]. *Journal of Donghua University (English Edition)*, 2019, 36(4): 369-376.

[11] HE Y X, ZENG Q N. Simulation study on frequency response of electroacoustic devices in active noise reduction [J]. *Computer Simulation*, 2021, 38(4): 168-171, 471. (in Chinese)

[12] QIU T S. The basic principle and method of time delay estimation [J]. *Marine Technology*, 1992(3): 17-26. (in Chinese)

[13] SAC/TC 17. Acoustics—materials for acoustical applications—determination of airflow resistance: GB/T 25077—2010 [S]. Beijing: Standards Press of China, 2010. (in Chinese)

[14] MA W T. Analysis and optimization of sound absorption and insulation properties of acoustic materials for vehicle high frequency noise [D]. Jilin: Jilin University, 2021. (in Chinese)


# 基于阻抗匹配的半主动吸声方法


朱从云*，张少奇，丁国芳

中原工学院 智能机电工程学院（工业设计学院），河南 郑州 450007



**摘　要：**主动吸声技术在降低低频声波方面表现出色，但在处理中高频声波时却表现不佳。为了提高中高频声波的吸声效果，提出了一种新型的半主动吸声方法。该方法调节吸声材料后扬声器的表面阻抗，将可控扬声器置于吸声材料后面，调节其表面阻抗，使其与空气的声阻抗达到最佳匹配，进而实现吸声性能的有效调控。利用 MATLAB 计算理论吸声系数，并将其与试验测得的吸声系数进行比较。结果表明，该方法可以在不断改变入射声波频率的情况下对吸声系数进行有效调整，使吸声系数始终处于最大值。



**关键词：**声阻抗；半主动吸声；刚性壁；空腔深度；吸声系数